



Kent Academic Repository

Nandi, Uttom, Mithu, Md. S. H., Hurt, Andrew P., Trivedi, Vivek and Douroumis, Dennis (2020) *Drug–Smectite Clay Amorphous Solid Dispersions Processed by Hot Melt Extrusion*. AAPS PharmSciTech, 21 . ISSN 1530-9932.

Downloaded from

<https://kar.kent.ac.uk/83441/> The University of Kent's Academic Repository KAR

The version of record is available from

<https://doi.org/10.1208/s12249-020-01813-x>

This document version

Author's Accepted Manuscript

DOI for this version

Licence for this version

UNSPECIFIED

Additional information

Versions of research works

Versions of Record

If this version is the version of record, it is the same as the published version available on the publisher's web site. Cite as the published version.

Author Accepted Manuscripts

If this document is identified as the Author Accepted Manuscript it is the version after peer review but before type setting, copy editing or publisher branding. Cite as Surname, Initial. (Year) 'Title of article'. To be published in *Title of Journal*, Volume and issue numbers [peer-reviewed accepted version]. Available at: DOI or URL (Accessed: date).

Enquiries

If you have questions about this document contact ResearchSupport@kent.ac.uk. Please include the URL of the record in KAR. If you believe that your, or a third party's rights have been compromised through this document please see our [Take Down policy](https://www.kent.ac.uk/guides/kar-the-kent-academic-repository#policies) (available from <https://www.kent.ac.uk/guides/kar-the-kent-academic-repository#policies>).

1
2
3
4
5
6
7
8
9
10
11
12
13
14
15
16
17
18
19
20
21
22
23

Drug – smectite clay amorphous solid dispersions processed by Hot Melt Extrusion

Uttom Nandi^{1,2}, Md. S.H. Mithu^{1,2}, Andrew P. Hurt¹, Vivek Trivedi³,
Dennis Douroumis^{1,2}

¹Faculty of Engineering and Science, School of Science, University of Greenwich, Chatham Maritime, Chatham, Kent ME4 4TB, UK

²CIPER Centre for Innovation and Process Engineering Research, Kent, ME4 4TB, UK

³Medway School of Pharmacy, University of Kent, Central Avenue, Chatham Maritime, Canterbury, Kent ME4 4TB, UK

¹ CIPER Centre for Innovation and Process Engineering Research, Kent, ME4 4TB, UK,

Email: d.douroumis@gre.ac.uk

24 ***Abstract***

25 The aim of this study was to investigate suitability of natural and synthetic smectite clay
26 matrices as a drug delivery carrier for the development of amorphous solid dispersions (ASD).
27 Indomethacin (IND) was processed with two different smectite clays, natural-magnesium
28 aluminium and synthetic-lithium magnesium sodium silicates, using Hot Melt Extrusion
29 (HME) to prepare solid dispersions. Scanning electron microscopy (SEM), Powdered X-ray
30 diffraction (PXRD), Differential scanning calorimetry (DSC) were used to examine the
31 physical form of the drug. Energy dispersive X-ray spectroscopy (EDX) was used to investigate
32 the drug distribution and Attenuated Total Reflectance-Fourier transform infrared (ATR-
33 FTIR) spectroscopic analysis was done to detect any chemical interaction between these two
34 kinds. Both, PXRD and DSC analysis showed that drug-clay solid dispersion contained IND
35 in amorphous form. Energy dispersive X-ray (EDX) analysis showed a uniform IND dispersion
36 in the extruded powders. ATR-FTIR data presented possible drug and clay interactions *via*
37 hydrogen bonding. *In-vitro* drug dissolution studies revealed a lag time of about two hours in
38 the acidic media and a rapid release of IND at pH 7.4. The work demonstrated that preparation
39 of amorphous solid dispersion using inorganic smectite clay particles can effectively increase
40 the dissolution rate of IND.

41 **KEYWORD:** Indomethacin, clay, hot-melt extrusion, dissolution, solid dispersion.

42

43

44

45

46

47

48

50 INTRODUCTION

51 To date, numerous drug molecules have been discovered with higher molecular weight, greater
52 lipophilicity, and minimal water solubility which often cause difficulties during their
53 pharmaceutical manufacturing process (1,2). Primarily, these factors are liable for an
54 inadequate drug dissolution and their limited bioavailability. At the same time, this rise of
55 poorly water soluble drugs also pushed for innovative strategies to overcome solubility related
56 issues *i.e.* salt formation (3), co-crystals (4), pro-drugs formation (5), solid lipid nanoparticle
57 (6), amorphous solid dispersion (7) *etc.* Among these, amorphous solid dispersion- invented
58 by Sekiguchi and Obi in 1961, has shown promising results for improving dissolution rates of
59 poorly water soluble compounds (8). This technique allows to disperse an insoluble drug in a
60 water soluble carrier at molecular level, enabling it to greatly enhance the total specific surface
61 area which ultimately increases the dissolution rate and bioavailability.

62 Clays are water soluble silicate compounds, generally used as an excipient in pharmaceutical
63 formulations *i.e.* lubricant, desiccant, disintegrant, diluent, binder, opacifier, as well as
64 emulsifying, thickening, isotonic agent, anticaking agent, flavour corrector and carrier of active
65 ingredients *etc.* (9–11). Among many varieties, smectite clays are particularly well known for
66 their water solubility, dispersivity, swelling capacity and relatively high specific surface area
67 (12). Takahashi and Yamaguchi believed that swelling ability of clay silicates and their
68 complex formation ability is beneficial to act as a drug carrier and solubilise poorly water-
69 soluble drugs (13). Authors prepared griseofluvin-clay hybrids with less than 5% clay complex
70 which demonstrated higher solubility compare to the pure drug. Goncalbes *et al.* also explored
71 the use of phyllosilicate clay mineral to increase the solubility of olanzapine (14). Prepared
72 phyllosilicate and olanzapine complex showed around 50% increase of dissolution rate within
73 first 60 minutes (min) of the study.

74 Smectite clays such as natural-Veegum (VF) and synthetic-laponite (LP) are also widely used
75 in the pharmaceuticals as stabilising and suspending agent, rheology modifier as well as texture
76 enhancer (15,16). Primarily, these high swelling clays contain Na⁺ ions in between their
77 interlayer spacing, enabling them to adsorb up to 32 layers of water molecules (17). Adebisi *et*
78 *al.* found that VF increases the dissolution rate of theophylline from the tablet matrices (15).
79 LP nanoparticles were used to enhance the solubility of itraconazole upto 75%, reported by
80 Jung *et al.* (18). Such investigations of clay mineral clearly indicating possibilities to improve
81 the dissolution rate of indomethacin (IND). The rationale for using clay silicates as a
82 dissolution rate enhancing component was the hydrophilic nature of silica particles. Silica
83 particles contain abundant hydroxyl groups and exceptionally high specific surface area that
84 enables drug particles to interact instantaneously with the water molecules through hydrogen
85 bonding. Bahl D. *et al.* co-grinded also IND with pharmaceutical silicates to enhance the
86 dissolution rate of the drug (19).

87 IND is a non-steroidal, anti-inflammatory drug belongs to BCS class II category with a
88 solubility of only 0.937 mg/L in water (20). Such a water insoluble drug often shows low
89 absorption and poor bioavailability. Also limited solubility of this drug may also increase the
90 residence time in the gastro-intestinal tract which may irritate the gastric mucosal layer (21).
91 Hence, IND formulation preparation with an improved dissolution rate is at utmost importance
92 to the pharmaceutical manufacturing industry.

93 The use of hot melt extrusion as a processing technology for the development of amorphous
94 solid dispersions is well – known in pharmaceutical industry. HME possesses many advantages
95 such as cost effective, high throughput, minimal waste loss and solvent free processing
96 technology. There are numerous studies where HME has been employed for preparing
97 amorphous solid dispersion with improved dissolution rates of poorly water soluble
98 compounds. Although polymeric solid dispersions of IND have been reported previously (22),

99 the efficacy of clay minerals as an inorganic carrier is yet to be explored. Hence, the current
100 study investigates the feasibility of natural and synthetic smectite clay silica particles for solid
101 dispersion of IND to improve the dissolution rates using TSE.

102 **MATERIALS AND METHODS**

103 **Materials**

104 Veegum F[®] (Magnesium aluminium metasilicate) and Laponite RDS[®] (Lithium magnesium
105 sodium silicate) clay minerals were kindly donated by Vanderbilt minerals llc. (USA) and BYK
106 additives ltd. (Germany) respectively. Indomethacin was purchased from Tokyo chemical
107 industries (Japan), with a purity of >98.0% and all the reagents were used as received. Other
108 chemical reagents such as hydrochloric acid, di-Potassium hydrogen orthophosphate,
109 Potassium di-hydrogen phosphate, acetonitrile (HPLC grade), Ortho-phosphoric acid were
110 purchased from Fisher scientific UK and used as received.

111 **Continuous processing of ASD using HME**

112 IND formulations shown in Table I. were blended using a Turbula TF2 Mixer (Switzerland)
113 for 10 min. Then solid dispersions of IND were prepared using a 10 mm Rondol Microlab twin
114 screw extruder (France) with a 25:1 L/D ratio. Standard screw configuration with two kneading
115 zones and three conveying zone was used to disperse solid drug materials in the clay matrices
116 (shown in Fig. 1). The extruder barrel has five different heating zones where 80- 140- 170-
117 170- 30 °C (from feed to die) temperature were used to established ASD. Extrusions were
118 processed using 25% or 0.1 kg/hr feed rate with a screw speed of 50 rpm.

119 **Table I.** Formulations used for continuous solid dispersion using HME

Formulation	IND (%)	VF (%)	LP (%)
VIN-20	20.0	80.0	-

VIN-40	40.0	60.0	-
LIN-20	20.0	-	80.0
LIN-40	40.0	-	60.0

120

*V- Veegum F, L- Laponite RDS, IN- Indomethacin



121

122

Fig. 1. Photograph of screw configuration.

123 **Morphology analysis of extrudates**

124 SEM was used to study the surface morphology of the prepared extrudates. All the samples
 125 were mounted on an aluminium stub using adhesive carbon tape and placed in a low humidity
 126 chamber prior to analysis. Samples were then examined using a Cambridge Instruments (S630,
 127 UK), SEM operating at an accelerating voltage of 1.0 kV. Particle size distributions of the
 128 extruded powders were determined using a Mastersizer 2000 laser diffraction instrument
 129 (Malvern Instruments, UK) with a dry powder sample dispersion accessory (Scirocco 2000)
 130 and pressure at 2 bar and a vibration feed rate of 50%. Samples were examined in triplicate and
 131 Mastersizer 2000 software was used for data evaluation.

132 **PXRD analysis**

133 Crystalline structure of the pure and extruded materials were investigated using a Bruker D8
 134 Advance (Germany) X-ray powder diffractometer in 2-theta mode. The instrument was
 135 equipped with a copper anode at 40 KV, parallel beam Goebel mirror, 0.2 mm exit slit and a
 136 LynxEye position sensitive detector with 3° opening (Lynxiris at 6.5 mm). Each sample was

137 prepared using a PMMA (Poly-methyl-methacrylate) sample holder which was scanned from
138 2 to 56 °2θ with a step size 0.02 °2θ, counting time 0.1 s per step and a rotation of 15 rpm.

139 **DSC analysis**

140 Thermal analysis were done using a Mettler-Toledo 823e (Switzerland) differential scanning
141 calorimeter on the drug and extruded samples. About 4 mg of samples were placed in a sealed
142 aluminium pan with pierced lids. Prepared samples were heated from 30 to 230 °C at a heating
143 rate of 10 °C/min under dry nitrogen atmosphere.

144 **ATR-FTIR analysis**

145 Pure drug, clays and extruded formulations were also separately compressed into a thin disk
146 using a SPECAC hydraulic press and investigated using a Perkin Elmer Spectrum Two ATR-
147 FTIR spectrometer (USA) between 450 and 4000 cm⁻¹ wavenumbers, with 10 scans at a
148 resolution of 8 cm⁻¹. Samples were then fixed onto an aluminium stub using double sided
149 carbon adhesive tape for elemental analysis using Energy dispersive X-ray (EDX)
150 spectroscopy.

151 **EDX analysis**

152 EDX spectroscopy was obtained using a JEOL JSM- 5310LV (JAPAN) instrument.
153 Micrographs were collected at 20 kV accelerating voltage, 20 mm working distance, 15 spot
154 size and using a backscattered electron detector. Elemental mapping was also studied using an
155 Aztec X-ray microanalysis system with X-Max^N detector from Oxford instrument (UK).

156 ***In-vitro* dissolution study**

157 Release of IND from the clay matrices were also examined using a Varian 705 DS (USA)
158 paddle apparatus at 100 rpm and 37 °C. At first, 750 mL 0.1 N HCl solution of pH 1.2 were
159 used to study the drug release for 2 hr. After that 150 mL of phosphate buffer was added and

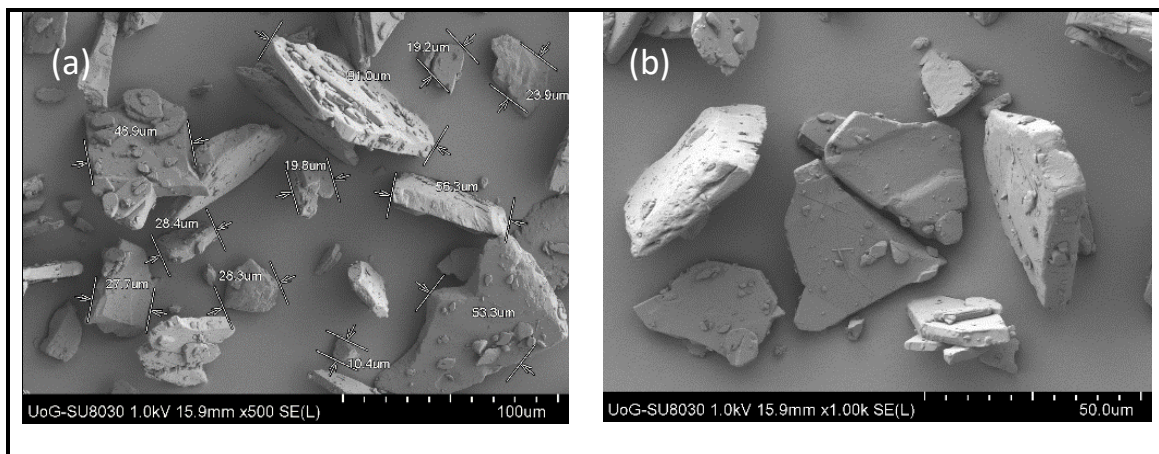
160 pH was adjusted to 7.4 using NaOH solution. Samples were collected at 15, 30, 60, 90, 120
161 min time interval from both pH and dissolution studies were also performed in triplicate.
162 Samples were then analysed using a high performance liquid chromatographic system provided
163 by Agilent Technologies, 1200 series (USA). IND was analysed using a HYCHROME
164 S50DS2-4889 (5×150×4 mm) column and an UV detector at a wavelength of 214 nm. The
165 mobile phase were prepared using acetonitrile: water: Ortho-phosphoric acid (49.5: 49.3: 0.2
166 v/v) and pumped at a flow rate of 1.5 mL/min. Abovementioned specification showed a 112 to
167 114 bar of column back pressure with a retention time of 3.00 ± 0.1 min. Calibration curve was
168 also prepared using 20, 40, 60, 80 and 100 µg/mL concentrated ethanolic solution of IND.

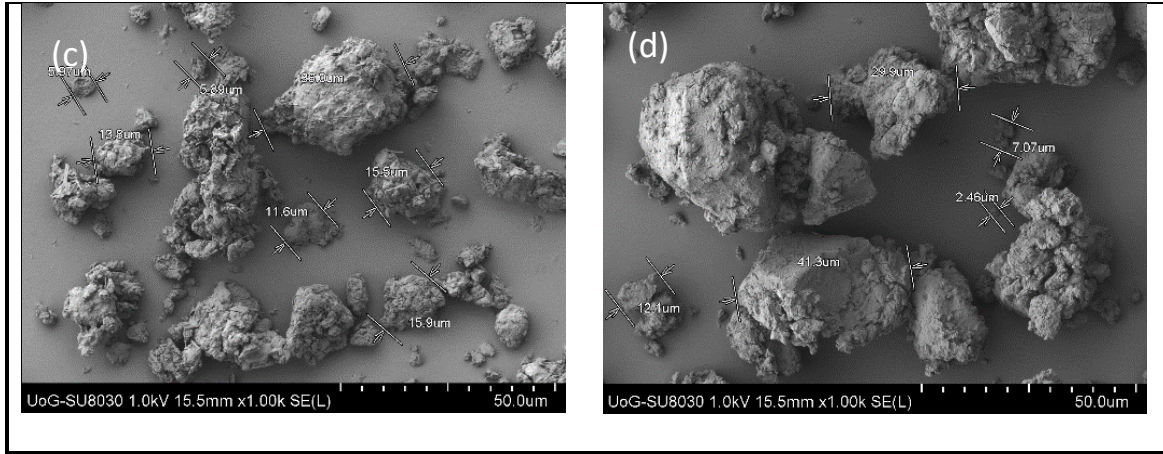
169 **RESULTS AND DISCUSSIONS**

170 In the current study, solid dispersions of IND in inorganic clay silicates were prepared by HME
171 and the suitability of clay silicates were also investigated as a carrier for poorly water-soluble
172 pharmaceutical actives. To optimise the processing conditions, various parameters such as
173 temperature, screw speed, feed rate were taken into careful considerations. Extrusion
174 temperature profile optimisation played a key role in the development of ASDs. Formulations
175 were also designed carefully to investigate the efficiency of HME processing on layered clay
176 silicates and drug molecules. Literature suggests, ASD prepared with HME technology
177 contains amorphous form of drug particles with a higher Gibbs free energy (23,24). In this
178 study, both natural and synthetic grades of hydrophilic smectite clays were used to increase the
179 wettability of IND leading to an improved drug dissolution rate. The drug and clay ratio was
180 further investigated to evaluate the effect on the dissolution rate improvement. The absence of
181 the die during extrusion led to the formation of free-flowing extruded powders in the form of
182 micro-particles which in turn reduced downstream processing. The powders were collected for
183 further physicochemical characterisation with no need for milling.

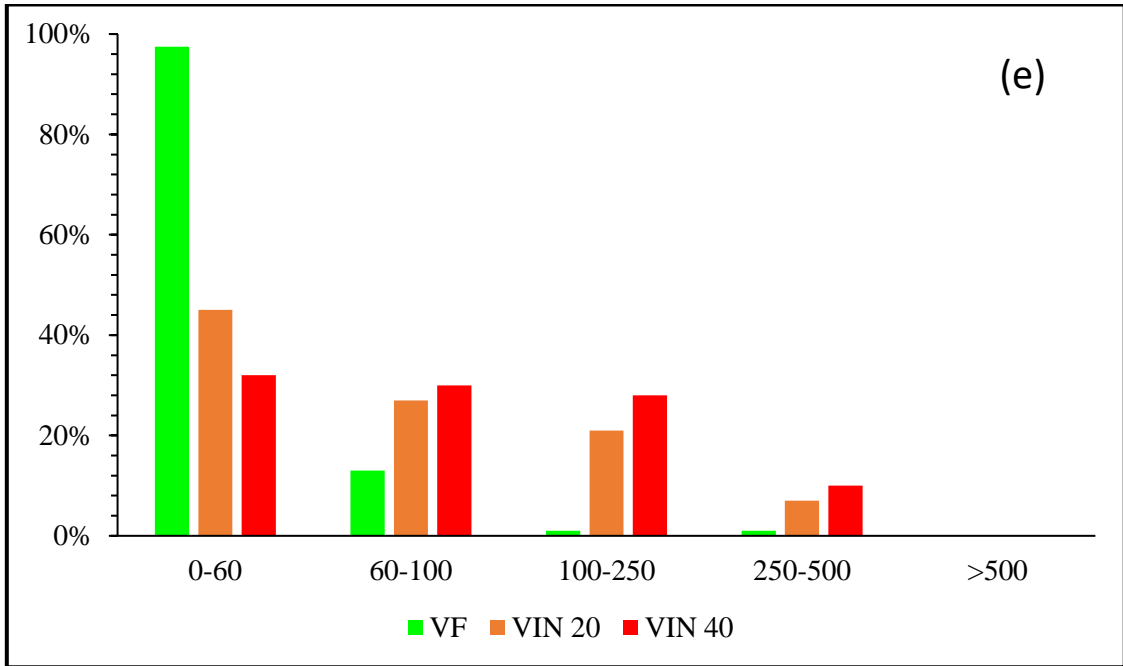
184 **Morphology analysis of extrudates**

185 The morphology of bulk drug and extruded formulations were analysed using SEM. Fig. 2. (a,
186 b) shows bulk IND particles which present plate-shape morphology. On the other hand, in Fig.
187 2. (c, d) the obtained solid dispersions showed the absence of crystalline IND as a result of the
188 extrusion process optimisation. This suggests the adsorption of melted drug molecules in the
189 silica porous network which not only facilitates the transformation of drug into amorphous
190 state but also result in improved powder flowability for the development of the finished dosage
191 form *i.e.* tablet preparation using direct compression method or capsules preparation (25). In
192 addition, the extruded dispersions appear as granular micro-agglomerates due to the absence
193 of the extrusion die. Extruded powders were then analysed using particle size analyser and
194 results has been presented in Fig. 2. (e, f). As it can be seen a large percentage of fine particles
195 was observed in the bulk clays prior to extrusion processing. In the drug loaded clays, a
196 significant reduction of the fines was detected, and the formation of larger agglomerates took
197 place in agreement with SEM analysis. In Fig. 2. e, can also be seen that higher drug loadings
198 (40%) facilitated the formation of larger granules with sizes varying from 100 – 500 μm .

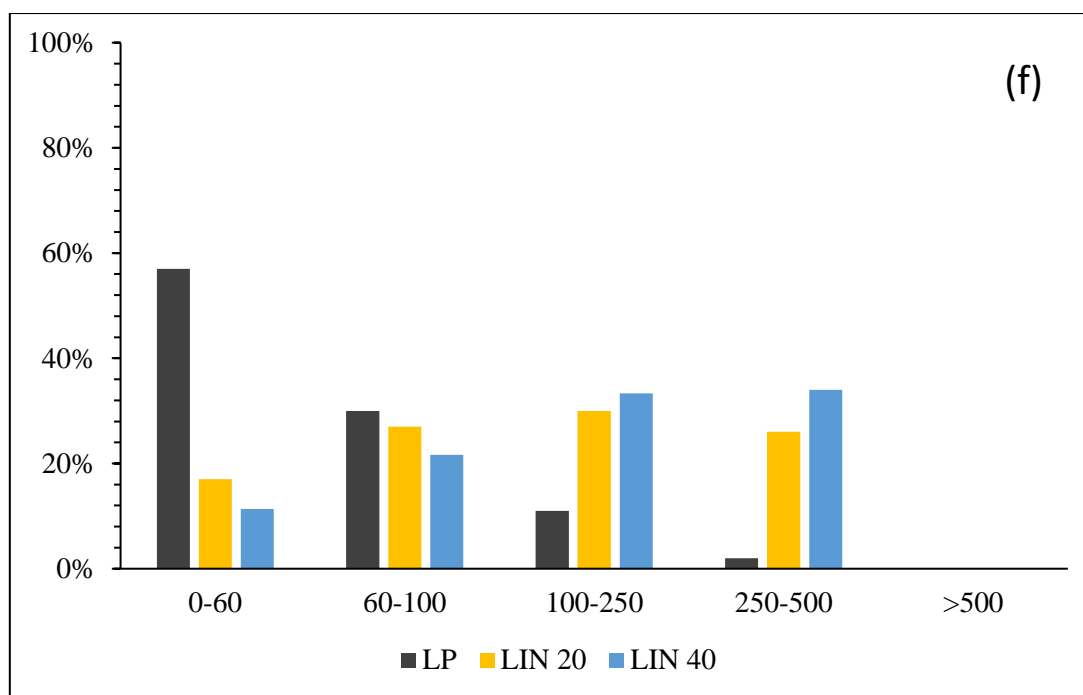




199
200



201



202

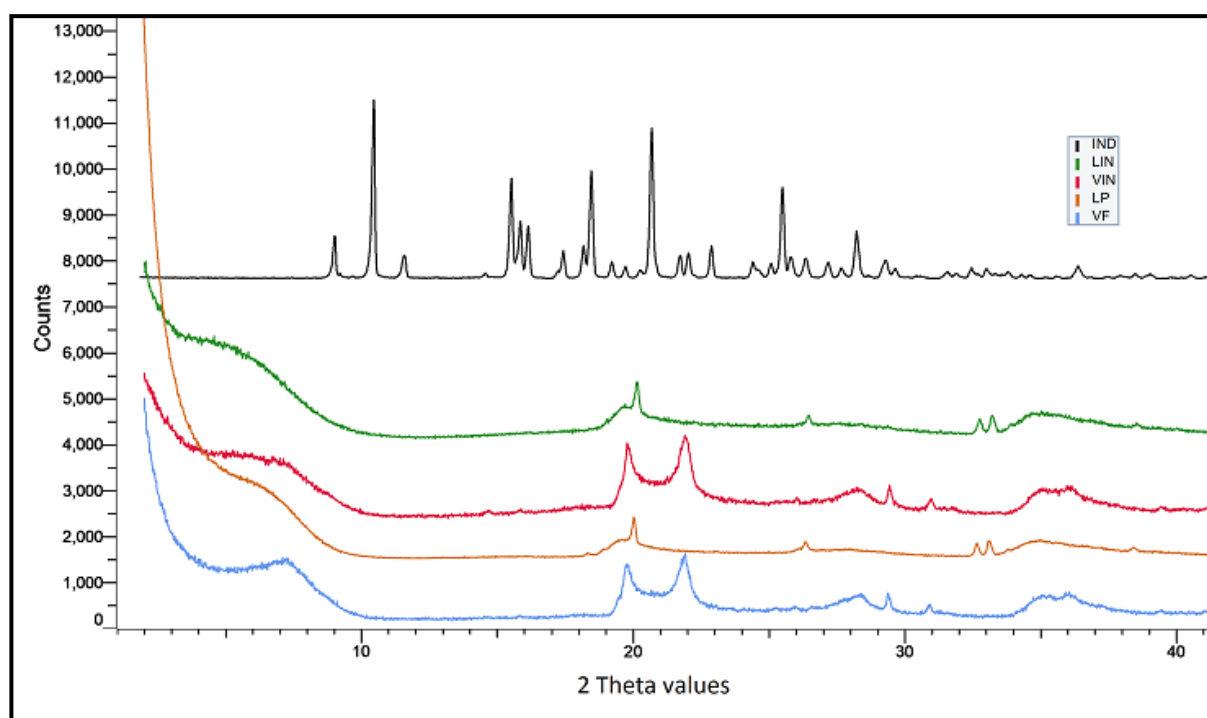
203 **Fig. 2.** (Top) SEM micrographs of (a-b) pure IND, c- VIN and d- LIN extruded formulations.

204 (Bottom) Particle size distribution of VIN, LIN extruded formulations against pure clay.

205 **PXRD analysis**

206 The physical state of the crystalline drug, clay and their extruded formulations were examined
 207 using PXRD analytical technique and shown in Fig. 3. Diffractogram of crystalline IND
 208 showed peaks with sharp intensity at 9.1, 10.6, 11.7, 15.8, 18.6, 20.8, 25.6 and 28.3 °2θ. Pure
 209 clays, VF and LP also showed their primary peaks at 7.4, 19.9, 21.9 °2θ and 6.5, 20.1, 33.3 °2θ
 210 respectively. Interlayer spacing for pure VF at 7.4 °2θ= 11.9 Å and LP at 6.5 °2θ= 13.6 Å was
 211 found using Bragg's law ($n\lambda=2d\sin\theta$). Although the interlayer spacing of anhydrous smectite
 212 clay should be ~ 10 Å, presence of homogeneous water molecules increases the interlayer
 213 spacing between two aluminosilicate sheets (26). The broad interlayer spacing also indicates
 214 the poor organisation of silicate layers in the structure. PXRD pattern of VIN and LIN
 215 formulations showed higher basal spacing compare to the pure clays. In particular, the basal
 216 spacing of VIN was indistinguishable in obtained the diffractogram. The IND – VIN and IND
 217 – LIN extruded formulation did not present any intensity peaks related to bulk IND. These

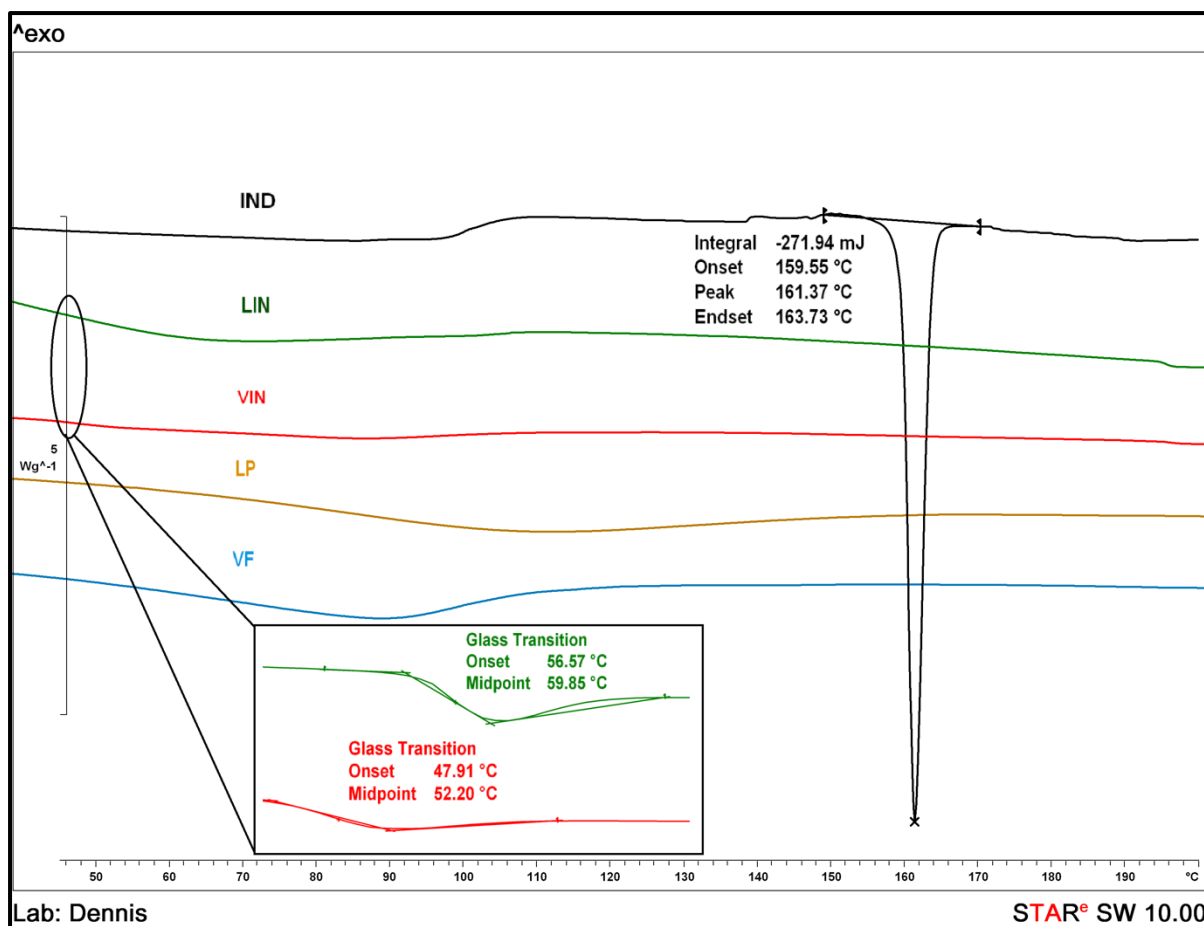
218 results suggest the formation of amorphous solid dispersions probably due to stronger
219 interactions between the drug and the clay at molecular level. Interestingly, the extruded
220 formulations appeared partially amorphous when extrusion temperatures were set below 160
221 °C. Stability studies were also performed at 25 °C/ 60% RH for 12 months and showed that
222 extruded IND-silicate dispersions were relatively stable with no more than 10±2% increase in
223 their crystallinity compared to fresh extruded batches.



224
225 **Fig. 3.** PXRD diffractograms of bulk IND, smectite clays and extruded formulations.

226 DSC analysis

227 Thermal transitions of bulk drug, clay and extruded formulations were studied using DSC
228 analysis shown in Fig. 4. The IND thermogram showed a sharp endothermic peak at 162 °C
229 representing the melting point of the pure crystalline IND (21,27). In contrast, both of the clays
230 did not present any melting endotherms within the investigated temperature range. However,
231 both VF and LP showed endothermic events at 35-125 °C and 35-165 °C respectively which
232 corresponds to the removal of the surface bound water molecules from the clay (28).



233

234

Fig. 4. Thermal transitions of pure IND, VF, LP, VIN and LIN extruded formulations.

235

Similarly, thermograms of VIN and LIN extruded formulations presented water loss at 30-110

236

°C with lower enthalpy values due to the HME processing at 170 °C. Fig. 4 also shows that the

237

absence of IND melting endothermic peak in VIN and LIN formulations (22,27). Most

238

importantly, the VIN and LIN thermograms presented endothermic events at 47.91 and 56.57

239

°C respectively which might correspond to the drug's T_g where for the amorphous IND is

240

around at 46 °C. However, the observed endothermic events showed a shift of T_g to higher

241

temperatures which is not unusual and it has been reported that clays can shift glass transitions

242

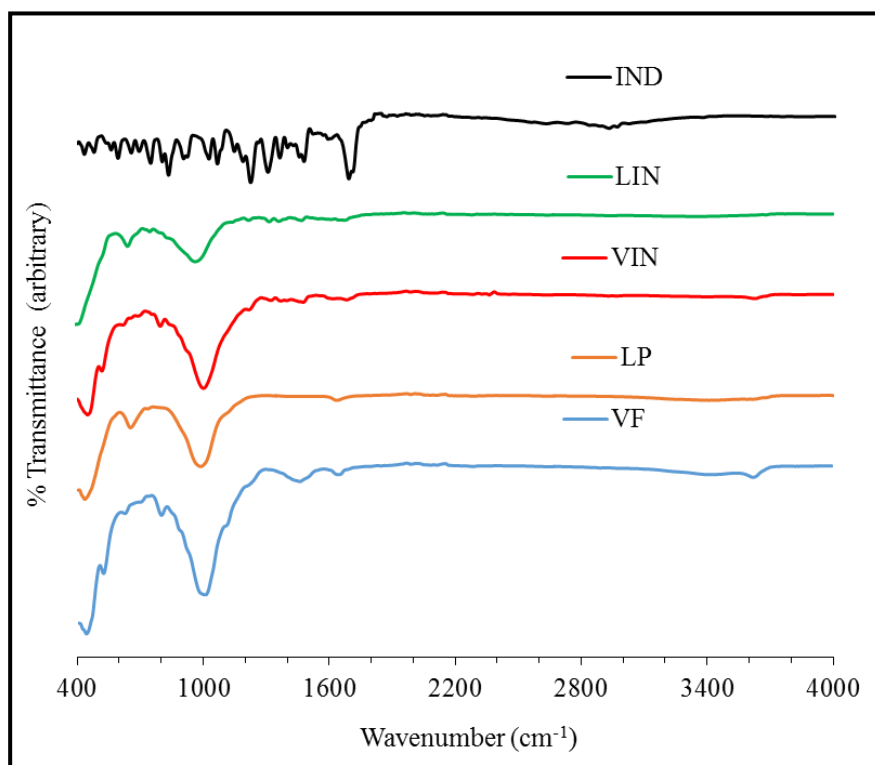
of drug or polymeric blends (29,30).

243

244

245 **ATR- FTIR spectroscopic analysis**

246 ATR-FTIR spectra of pure drug, clays and drug-clay complexes are shown in Fig. 5. Both VF
247 and LP clays showed a broad band at 3400 cm^{-1} due to $-\text{OH}$ stretching band for interlayer
248 adsorbed water (31). The band around 3640 and 3690 cm^{-1} is due to the Al-OH and Si-OH
249 stretching respectively (32). The presence of several hydroxyl groups in the clay contributes to
250 the broadness of this stretching band. The absorption peak at 1650 cm^{-1} belongs to the bending
251 mode of hydroxyl group of the interlayer water molecules.



252

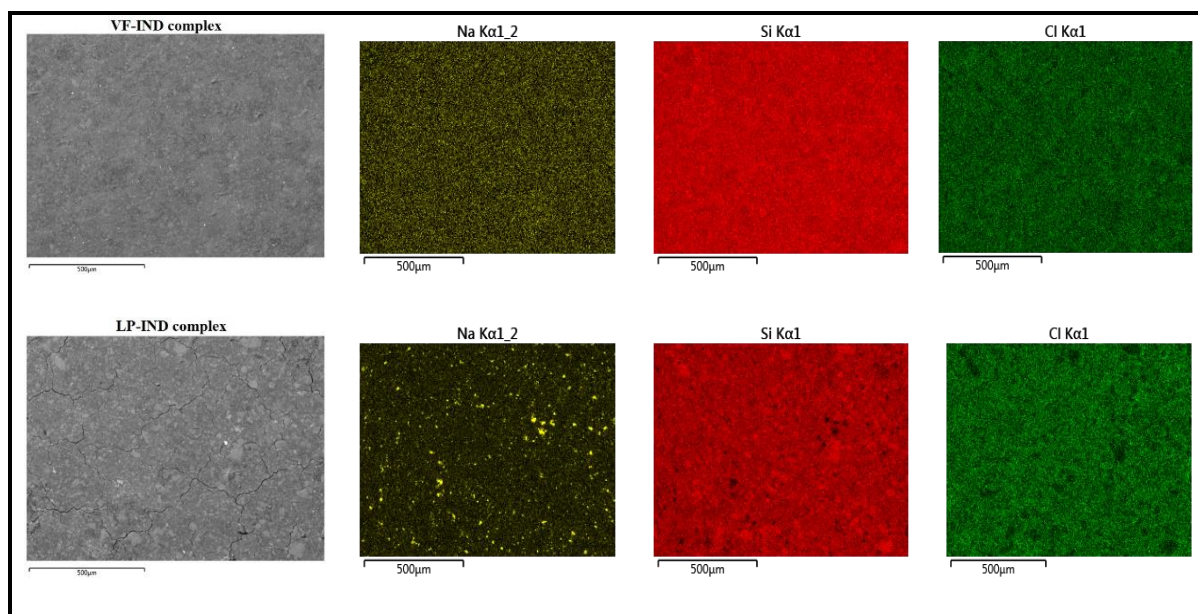
253 **Fig. 5.** ATR-FTIR spectrum of pure IND, VF, LP and VIN, LIN extruded formulations.

254 The characteristic peak at 1000 cm^{-1} is related to the Si-O stretching vibration of the clay
255 (33,34). IND spectra showed C=O stretching vibration in the range of $1600\text{-}1750\text{ cm}^{-1}$ while
256 the peak at 1694 cm^{-1} is the characteristic of polymorphic Form – I of the drug substance (35).
257 IND presents also a carbonyl and benzoyl groups at 1694 cm^{-1} and 1688 cm^{-1} respectively.
258 Extruded VIN and LIN formulations showed that stretching vibration of IND at 1694 cm^{-1} was

259 shifted to around 1670 cm^{-1} which indicates that crystalline structure of IND has transformed
260 to the amorphous state (36,37). The changes in the carbonyl spectral region indicate an
261 alteration in the drug's molecular state where the shifting of carbonyl stretching is attributed to
262 the disruption of IND-IND molecular interactions in its crystal structure. The bonding energy
263 of carbonyl oxygen from IND decreases after adsorption of the drug onto the clay silicate,
264 resulting a weakening of the carbonyl peak at 1670 cm^{-1} . Finally, the shift of the carbonyl band
265 suggests possible H-bonding formation with the clay platelets (35).

266 **EDX spectroscopic analysis**

267 Microscopic analysis and elemental mapping were studied for the drug-clay solid dispersions
268 to evaluate the presence and distribution of IND in the clay matrices. As shown in Fig. 6,
269 micrographs were collected using back-scattered electrons and corresponding EDX elemental
270 maps of Na, Si and Cl showing variation of clay and drug distribution within the extruded
271 samples. Clays such as VF primarily contain Na, Mg, Ca, Si and LP contains Na, Mg, Li, Si
272 atoms in its structure (38,39). Heavier elements in a molecule appears brighter in a
273 backscattered electron micrograph compared to the lighter atoms. The above micrographs in
274 grayscale clearly explains the homogeneous distribution of VF and agglomerated LP clay
275 distribution in the VIN and LIN dispersions respectively. X-ray elemental mapping of Na and
276 Si (presented in yellow and red respectively, top) also confirmed homogenous distribution of
277 VF in the VIN complex. In contrast, LIN extrudates exhibited a more inhomogeneous
278 dispersion with areas high in Na and P (P EDX map not shown) indicating an additional phase
279 in the drug-clay matrix (shown in the Na and Si ion map, bottom).



280 **Fig. 6.** Elemental analysis of extruded formulations, collected using SEM (Top – BSE
 281 micrograph of VIN extrudates and its Na, Si, Cl mapping; Bottom – BSE micrograph of LIN
 282 extrudates and its Na, Si, Cl mapping)

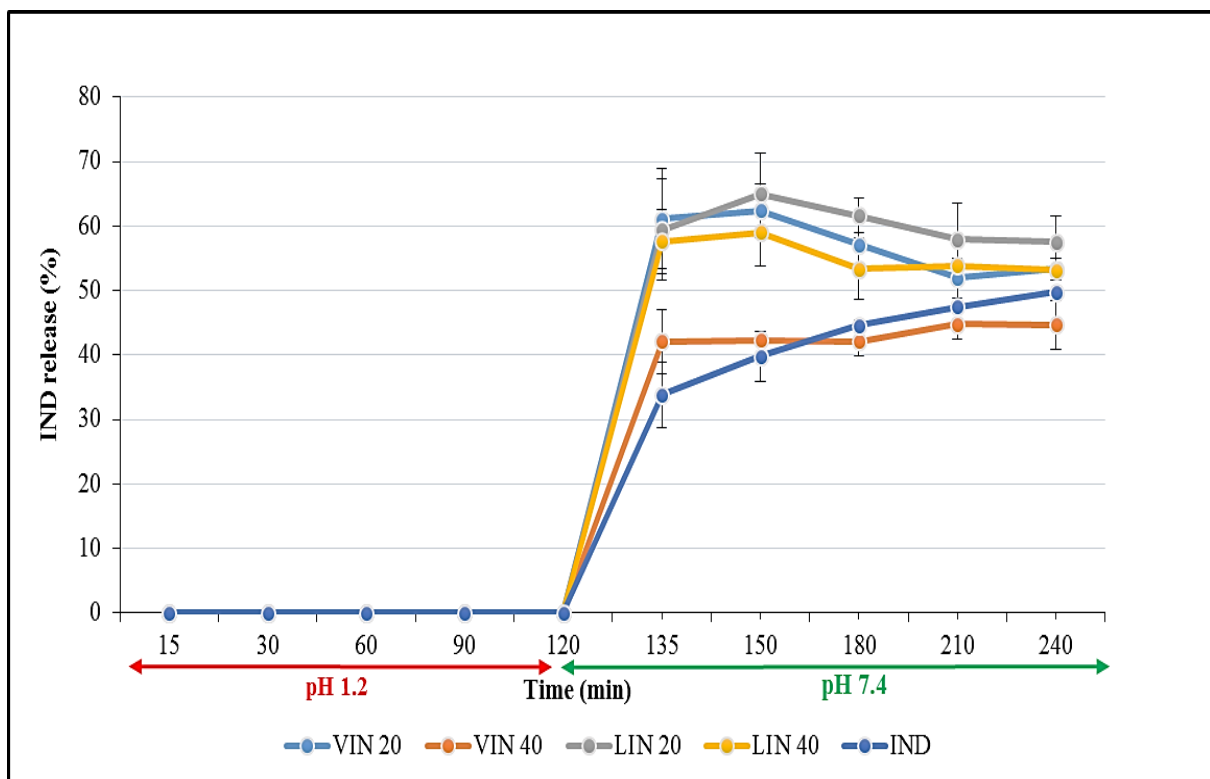
283 Furthermore, chemical structure of IND contains chlorine (Cl) atom in its chemical structure
 284 while both the clays have no Cl present. Therefore, an X-ray elemental mapping of Cl as a
 285 marker will reveal the homogeneity of drug distribution. Mapping data of Cl (presented in green)
 286 shows that VIN extrudate contains uniform drug distribution where else LIN complex shows
 287 presence of dark area, indicating a less uniform clay drug distribution. These type of poly-
 288 dispersions may be minimised by optimising the processing parameters during extrusion.

289 ***In-vitro* dissolution study**

290 The *in-vitro* dissolution study was conducted using extruded drug-clay complex formulations
 291 and the bulk drug substance. The results of the study are shown in Fig. 7. The use of smectite
 292 clays for the development of amorphous solid dispersions facilitated controlled release of the
 293 drug substance for both formulations. As shown in Fig. 7, dissolution studies presented a lag
 294 time with no IND release in acidic (pH 1.2) dissolution media. After 120 min, the pH was

295 adjusted to 7.4 and bulk IND presented 33% and 50% drug release at 15 min and 120 min
296 respectively.

297 In contrast, clay-drug complexes showed a burst release of IND from the clay matrices at 135
298 min. The VIN 20 and LIN 20 solid dispersions showed almost 60% drug release within the first
299 15 min. At higher drug loadings, LIN 40 also presented rapid dissolution rates at 57% while
300 the VIN 40 at 47% respectively. This could be attributed to the higher particle size of VIN 40
301 and LIN 40 formulations.



302

303 **Fig. 7.** *In-vitro* dissolution profiles of pure IND and HME extruded formulations at pH 1.2 (0-120
304 min) and pH 7.4 (120-240 min).

305 Overall, the increase of dissolution rates could be attributed to several factors such as the
306 amorphous form of IND molecules, particle size and H-bonding due to the drug-clay
307 interactions. The clay particles may have shown some ionic interactions between adsorbate
308 and adsorbent surface during the release study at pH 7.4 (40,41). As IND is a weak acid, the

309 highly negative surface charge of the clay at pH 7.4, might have induced dissociation of IND
310 molecule resulting in burst release. In addition, the negatively charged smectite particles
311 (negative charges on the border plane of the smectite layers) may have also created repulsive
312 forces to IND that led to drug desorption from the clay matrices (42,43).

313 Although, a burst release of IND was initially observed, it can be seen in Fig. 7 that IND
314 dissolution rates decreased over time. This can be attribute to possible IND recrystallisation
315 where the amorphous drug crystallized in the dissolution media due to the generated
316 supersaturation solution (25,44). Nevertheless, it can be concluded that the dissolution rate
317 improvement of IND was achieved not only by conversion of its physical form but also through
318 the specific chemical environment created by clay silicates.

319 CONCLUSIONS

320 The current study about smectite clays were introduced as an alternative drug carrier for the
321 formation of IND amorphous solid dispersions. PXRD and DSC studies demonstrated that
322 IND was converted into amorphous form while EDX analysis revealed excellent IND content
323 uniformity in the clay matrices due to extrusion processing. The extruded ASD presented
324 controlled release with rapid IND dissolution rates in alkaline media for drug loadings varying
325 from 20 to 40%. In conclusion, smectite clays can be used as a drug carriers for the
326 development of ASDs at up to 40% high drug loadings.

327 DISCLOSURE STATEMENT

328 The authors report no conflict of interests.

329 ACKNOWLEDGEMENTS

330 This project has received funding from the Interreg 2 Seas programme 2014-2020 co-funded
331 by the European Regional Development Fund under subsidy contract 2S01-059_IMODE.

332 **REFERENCES**

- 333 1. Keserü GM, Makara GM. The influence of lead discovery strategies on the properties
334 of drug candidates. *Nat Rev Drug Discov.* 2009;8(3):203–12.
- 335 2. Lipinski CA. Drug-like properties and the causes of poor solubility and poor
336 permeability. *J Pharmacol Toxicol Methods.* 2000;44(1):235–49.
- 337 3. Hiendrawan S, Widjojokusumo E, Veriansyah B, Tjandrawinata RR. Pharmaceutical
338 salts of carvedilol: polymorphism and physicochemical properties. *AAPS*
339 *PharmSciTech.* 2017;18(4):1417–25.
- 340 4. Box KJ, Comer J, Taylor R, Karki S, Ruiz R, Price R, et al. Small-scale assays for
341 studying dissolution of pharmaceutical cocrystals for oral administration. *AAPS*
342 *PharmSciTech.* 2016;17(2):245–51.
- 343 5. Upadhye SB, Kulkarni SJ, Majumdar S, Avery MA, Gul W, ElSohly MA, et al.
344 Preparation and Characterization of Inclusion Complexes of a Hemisuccinate Ester
345 Prodrug of Δ 9-Tetrahydrocannabinol with Modified Beta-Cyclodextrins. *Aaps*
346 *Pharmscitech.* 2010;11(2):509–17.
- 347 6. Wang L, Li H, Wang S, Liu R, Wu Z, Wang C, et al. Enhancing the antitumor activity
348 of berberine hydrochloride by solid lipid nanoparticle encapsulation. *Aaps*
349 *Pharmscitech.* 2014;15(4):834–44.
- 350 7. Haser A, Zhang F. New strategies for improving the development and performance of
351 amorphous solid dispersions. *Aaps Pharmscitech.* 2018;19(3):978–90.
- 352 8. Sekiguchi K, Obi N. Studies on Absorption of Eutectic Mixture. I. A Comparison of the
353 Behavior of Eutectic Mixture of Sulfathiazole and that of Ordinary Sulfathiazole in Man.
354 *Chem Pharm Bull.* 1961;9(11):866–72.

- 355 9. Abend S, Lagaly G. Sol–gel transitions of sodium montmorillonite dispersions. Appl
356 Clay Sci. 2000;16(3–4):201–27.
- 357 10. Carretero MI, Pozo M. Clay and non-clay minerals in the pharmaceutical industry Part
358 I. Excipients and medical applications. Appl Clay Sci. 2009;46:73–80.
- 359 11. Viseras C, Lopez-Galindo A. Pharmaceutical applications of some Spanish clays
360 (sepiolite, palygorskite, bentonite): some preformulation studies. Appl Clay Sci.
361 1999;14(1–3):69–82.
- 362 12. Carretero MI, Pozo M. Clay and non-clay minerals in the pharmaceutical industry. Part
363 I. Excipients and medical applications. Appl Clay Sci. 2009;46(1):73–80.
- 364 13. Adebisi AO, Conway BR, Asare-Addo K. The influence of fillers on theophylline
365 release from clay matrices. Am J Pharmacol Sci. 2015;3(5):120–5.
- 366 14. Gonçalves MLCM, Lyra MAM, Oliveira FJVE, Rolim LA, Nadvorny D, Vilarinho
367 ACSG, et al. Use of phyllosilicate clay mineral to increase solubility olanzapine. J
368 Therm Anal Calorim. 2017;127(2):1743–50.
- 369 15. Adebisi AO, Conway BR, Asare-Addo K. The influence of fillers on theophylline
370 release from clay matrices. Am J Pharmacol Sci. 2015; 2016:120–5.
- 371 16. Kim MH, Choi G, Elzatahry A, Vinu A, Choy Y Bin, Choy JH. Review of clay-drug
372 hybrid materials for biomedical applications: Administration routes. Clays Clay Miner.
373 2016;64(2):115–30.
- 374 17. McPhee C, Reed J, Zubizarreta I. Core Sample Preparation. In: Developments in
375 Petroleum Science. Elsevier; 2015. p. 135–79.
- 376 18. Jung H, Kim H, Bin Y, Hwang S, Choy J. Laponite-based nanohybrid for enhanced
377 solubility and controlled release of itraconazole. Int J Pharm. 2008;349:283–90.

- 378 19. Bahl D, Hudak J, Bogner RH. Comparison of the ability of various pharmaceutical
379 silicates to amorphize and enhance dissolution of indomethacin upon co-grinding.
380 Pharm Dev Technol. 2008;13(3):255–69.
- 381 20. Löbenberg R, Amidon GL. Modern bioavailability, bioequivalence and
382 biopharmaceutics classification system. New scientific approaches to international
383 regulatory standards. Eur J Pharm Biopharm. 2000;50(1):3–12.
- 384 21. Alsaidan SM, Alsughayer AA, Eshra AG. Improved Dissolution Rate of Indomethacin
385 by Adsorbents. Drug Dev Ind Pharm [Internet]. 1998 Jan 1;24(4):389–94.
- 386 22. Zhang W, Zhang C ning, He Y, Duan B yan, Yang G yi, Ma W dong, et al. Factors
387 Affecting the Dissolution of Indomethacin Solid Dispersions. AAPS PharmSciTech.
388 2017;18(8):3258–73.
- 389 23. Hwang I, Kang C-Y, Park J-B. Advances in hot-melt extrusion technology toward
390 pharmaceutical objectives. J Pharm Investig. 2017;47(2):123–32.
- 391 24. Prasad D, Chauhan H, Atef E. Amorphous stabilization and dissolution enhancement of
392 amorphous ternary solid dispersions: combination of polymers showing drug–polymer
393 interaction for synergistic effects. J Pharm Sci. 2014;103(11):3511–23.
- 394 25. Maniruzzaman M, Nair A, Scoutaris N, Bradley MSA, Snowden MJ, Douroumis D.
395 One-step continuous extrusion process for the manufacturing of solid dispersions. Int J
396 Pharm. 2015;496(1):42–51.
- 397 26. Villar M V, Gómez-Espina R, Gutiérrez-Nebot L. Basal spacings of smectite in
398 compacted bentonite. Appl Clay Sci. 2012;65:95–105.
- 399 27. El-Badry M, Fetih G, Fathy M. Improvement of solubility and dissolution rate of
400 indomethacin by solid dispersions in Gelucire 50/13 and PEG4000. Saudi Pharm J.

- 401 2009;17(3):217–25.
- 402 28. Grim RE, Bradley WF. Investigation of the effect of heat on the clay minerals illite and
403 montmorillonite. *J Am Ceram Soc.* 1940;23(8):242–8.
- 404 29. Corcione CE, Maffezzoli A. *Thermochimica Acta* Glass transition in thermosetting clay-
405 nanocomposite polyurethanes. 2009;485:43–8.
- 406 30. Qazvini NT, Chehrazi E. Glass transition behavior and dynamic fragility of PMMA-
407 SAN miscible blend-clay nanocomposites. *J Macromol Sci Part B Phys.*
408 2011;50(11):2165–77.
- 409 31. Tabak A, Yilmaz N, Eren E, Caglar B, Afsin B, Sarihan A. Structural analysis of
410 naproxen-intercalated bentonite (Unye). *Chem Eng J.* 2011;174(1):281–8.
- 411 32. Kevadiya BD, Patel HA, Joshi G V, Abdi SHR, Bajaj HC. Montmorillonite-Alginate
412 Composites as a Drug delivery System : Intercalation and In vitro Release of Diclofenac
413 sodium. *Indi.* 2010;72(6):732–7.
- 414 33. Patel HA, Somani RS, Bajaj HC, Jasra R V. Preparation and characterization of
415 phosphonium montmorillonite with enhanced thermal stability. *Appl Clay Sci.*
416 2007;35(3–4):194–200.
- 417 34. Ghadiri M, Chrzanowski W, Lee WH, Fathi A, Dehghani F, Rohanizadeh R. Physico-
418 chemical, mechanical and cytotoxicity characterizations of Laponite®/alginate
419 nanocomposite. *Appl Clay Sci.* 2013;85:64–73.
- 420 35. A RM, Kebriaee A, Keshavarz M, Ahmadi A, Mohtat B. Preparation and in-vitro
421 evaluation of indomethacin nanoparticles. 2010;18(3):185–92.
- 422 36. Fini A, Cavallari C, Ospitali F. Raman and thermal analysis of indomethacin/PVP solid
423 dispersion enteric microparticles. *Eur J Pharm Biopharm.* 2008;70(1):409–20.

- 424 37. Kocbek P, Baumgartner S, Kristl J. Preparation and evaluation of nanosuspensions for
425 enhancing the dissolution of poorly soluble drugs. *Int J Pharm.* 2006;312(1–2):179–86.
- 426 38. Jatav S, Joshi, M Y. Chemical stability of Laponite in aqueous media. *Appl Clay Sci.*
427 2014;97–98(August):72–7.
- 428 39. Trivedi V, Nandi U, Maniruzzaman M, Coleman NJ. Intercalated theophylline-smectite
429 hybrid for pH-mediated delivery. *Drug Deliv Transl Res.* 2018;8:1781–9.
- 430 40. Netpradit S, Thiravetyan P, Towprayoon S. Adsorption of three azo reactive dyes by
431 metal hydroxide sludge: effect of temperature, pH, and electrolytes. *J Colloid Interface*
432 *Sci.* 2004;270(2):255–61.
- 433 41. Tabak A, Eren E, Afsin B, Caglar B. Determination of adsorptive properties of a Turkish
434 Sepiolite for removal of Reactive Blue 15 anionic dye from aqueous solutions. *J Hazard*
435 *Mater.* 2009;161(2–3):1087–94.
- 436 42. Tabak A, Baltas N, Afsin B, Emirik M, Caglar B, Eren E. Adsorption of Reactive Red
437 120 from aqueous solutions by cetylpyridinium-bentonite. *J Chem Technol Biotechnol.*
438 2010;85(9):1199–207.
- 439 43. Tombacz E, Szekeres M. Colloidal behavior of aqueous montmorillonite suspensions:
440 the specific role of pH in the presence of indifferent electrolytes. *Appl Clay Sci.*
441 2004;27(1–2):75–94.
- 442 44. Alonzo DE, Zhang GGZ, Zhou D, Gao Y, Taylor LS. Understanding the behavior of
443 amorphous pharmaceutical systems during dissolution. *Pharm Res.* 2010;27(4):608–18.
- 444
- 445

446

447

448